Ab Initio Calculation of the Magnetic Exchange Interactions in (μ-Oxo)diiron(III) Systems Using a Broken Symmetry Wave Function

J. R. Hart and A. K. Rappé*

Department of Chemistry, Colorado State University, Fort Collins, Colorado 80523

S. M. Gorun*

Corporate Research Laboratories, Exxon Research and Engineering, Annandale, New Jersey 08801

T. H. Upton*

Products Research Division, Exxon Research and Engineering, Linden, New Jersey 07036

Received April 10, 1992

The results of broken symmetry ab initio unrestricted Hartree–Fock calculations are used to probe the angular and distance dependence of the magnetic coupling between a pair of iron centers bridged by an oxo ligand. The specific complex studied was $Na_2[Fe_2OCl_6]$. We find the magnetic interaction to be sensitive to the Fe–O distance but rather insensitive to the Fe–O–Fe angle. Further, we calculate J, the Heisenberg coupling constant, to be -170.0 cm^{-1}, when the Fe–O distance is 1.75 Å.

Introduction

Compounds which contain μ-oxo-bridged iron(III) have been studied extensively.[1,2] Proteins in oxygen carriers such as ribonucleotide reductase[3] and hemerythrins[4] contain these units. Several model complexes with the Fe–O–Fe core have been synthesized, and their structural and magnetic properties have been recorded. Each iron(III) center is found to be high-spin d^5, and the two couple antiferromagnetically in all known cases to produce a singlet ground state. Recently, a quantitative magneto–structural relationship has been found for a series of multiply bridged (μ-oxo) iron compounds which relates the magnetic coupling constant J to the "shortest superexchange pathway" between the iron centers and the bridge length.[5]

Calculations of the magnetic coupling constants for bridged transition metal dimers that consider only the interactions between the metal ions have been shown to be inadequate.[6] Contributions of orbitals of the bridging species must be taken into account. Calculations using perturbation theory on bridged copper d^9–d^9 dimers show that relaxing the orthogonality of the metal orbitals alone does not reproduce the experimental results.[6a-d] In fact, the calculated magnetic exchange constants at this level theory can be of the wrong sign; i.e., they are predicted to be ferromagnetic while these systems are found experimentally to be antiferromagnetic. Including the effects of the bridge lowers the singlet relative to the triplet enough so that the coupling constant is of the correct sign and order of magnitude.

This type of perturbation calculation is not commonly applied to systems with more than one magnetic orbital per metal ion. As the number of electrons per center increases, so does the size of the calculation. For bridged d^5 iron(III) systems, the size of a perturbation or (alternatively) a CI calculation necessary to describe them becomes unmanageable. In order to avoid this difficulty, Xα or local density functional (LDF) theory, based on unrestricted Hartree–Fock (UHF) wave functions, has been implemented for a number of sulfur-bridged iron systems.[7] Noodleman and Davidson[8] have argued that the broken symmetry wave function obtained via a UHF formalism contains the important bridge effect called ligand spin polarization.

There are two goals in this paper.[9] The first is to study the qualitative effect of systematic variations in geometric parameters on the magnetic exchange constant J. As a test case a singly bridged μ-oxo complex, $[Fe_2OCl_6]^{2-}$, has been chosen. The molecule $[Fe_2OCl_6]^{2-}$ has been structurally and magnetically characterized[10-12] in the presence of several different counterions. The second goal is to quantitatively compare the results of the Noodleman–Davidson approach discussed above against experimental measurements. Specifically, an effective J value is calculated using an open-shell restricted Hartree–Fock (RHF) wave function to describe the high-spin state and a broken

(1) Murray, K. S. *Coord. Chem. Rev.* **1974**, *12*, 1.
(2) Mukherjee, R. N.; Stack, T. D. P.; Holm, R. H. *J. Am. Chem. Soc.* **1988**, *110*, 1850.
(3) Scarrow, R. C.; Maroney, M. J.; Palmer, S. M.; Que, L., Jr.; Salowe, S. P.; Stubbe, J. *J. Am. Chem. Soc.* **1986**, *108*, 6832.
(4) Stenkamp, R. E.; Sieker, L. C.; Jensen, L. H. *J. Am. Chem. Soc.* **1984**, *106*, 618.
(5) Gorun, S. M.; Lippard, S. J. *Inorg. Chem.* **1991**, *30*, 1626.
(6) (a) De Loth, P.; Cassoux, P.; Daudey, J. P.; Malrieu, J. P. *J. Am. Chem. Soc.* **1981**, *103*, 4007. (b) De Loth, P.; Daudey, J. P.; Astheimer, H.; Walz, L.; Haase, W. J. *J. Chem. Phys.* **1985**, *82*, 5048. (c) Astheimer, H.; Haase, W. *J. Chem. Phys.* **1986**, *85*, 1427. (d) Charlot, M. F.; Verdaguer, M.; Journaux, Y.; De Loth, P.; Daudey, J. P. *Inorg. Chem.* **1984**, *23*, 3802. (e) De Loth, P.; Karafiloglou, P.; Daudey, J. P.; Kahn, O. *J. Am. Chem. Soc.* **1988**, *110*, 5676.
(7) (a) Noodleman, L. *J. Chem. Phys.* **1981**, *74*, 5737. (b) Norman, J. G., Jr.; Ryan, P. B.; Noodleman, L. *J. Am. Chem. Soc.* **1980**, *102*, 4279. (c) Aizman, A.; Case, D. A. *J. Am. Chem. Soc.* **1982**, *104*, 3269. (d) Noodleman, L.; Baerends, E. J. *J. Am. Chem. Soc.* **1984**, *106*, 2316. (e) Noodleman, L.; Case, D. A.; Aizman, A. *J. Am. Chem. Soc.* **1988**, *110*, 1001.
(8) Noodleman, L.; Davidson, E. R. *Chem. Phys.* **1986**, *109*, 131.
(9) A preliminary account of this work has appeared in: Hart, J. R. Ph.D. Dissertation, Colorado State University, Fort Collins, CO, Feb 1990.
(10) (a) Alder, J.; Ensling, J.; Gutlich, P.; Bominaar, E.; Guillin, J.; Trautwein, A. X. *Rec. Trav. Chim. Pays-Bas*, **1987**, *106*, 34. (b) Alder, J.; Ensling, J.; Gutlich, P.; Bominaar, E. L.; Guillin, J.; Trautwein, A. X. *Hyperfine Interact.* **1988**, *49*, 869.
(11) Subsequent to the completion of this work, a reexamnation of the structural and magnetic data on the $[Fe_2OCl_6]^{2-}$ anion in the presence of several different counterions has been completed.[12] These new results show that within experimental error the magnetic coupling constant (~112 cm^{-1}) is independent of Fe–O–Fe angle, as predicted by our results.
(12) Haselhorst, G.; Wieghardt, K.; Keller, S.; Schrader, B. *Inorg. Chem.*, submitted for publication.

0020-1669/92/1331-5254$03.00/0 © 1992 American Chemical Society

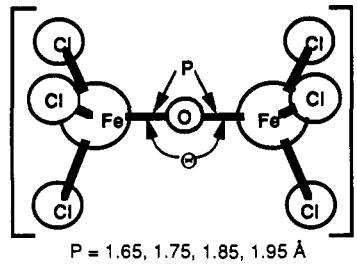

P = 1.65, 1.75, 1.85, 1.95 Å

Θ = 120°, 140°, 160°, 180°

(Sodium atoms not shown)

Figure 1. Geometries used for $[Fe_2OCl_6]^{2-}$.

Table I. Experimental J Values from Ref 10

molecule	Fe–O–Fe angle (deg)	Fe–O dist (Å)	J (cm^{-1})
$[Fe(bpy)_3][Fe_2OCl_6]$	148.1	1.765	−133.8
$(Hpy)_2[Fe_2OCl_6]\cdot py$	153.6	1.755	−126.8
$(Et_3NCH_2Ph)_2[Fe_2OCl_6]$	155.4	1.755	−146.1
$[(Ph_3P)_2CSe]_2[Fe_2OCl_6]$	180.0	1.752	−190.3

symmetry UHF wave function to describe the low-spin state. The open-shell high-spin wave function is an eigenfunction of spin with $S = 5$ ($\langle S^2 \rangle = 30$), while the broken symmetry wave function is not. It possesses an expectation value for S^2 of about 5, indicating significant spin contamination. While the broken symmetry state is not a pure spin singlet, we can use Noodleman's simple interpolation scheme to calculate an effective J value. This method is obviously an approximation, but as discussed below it yields structural (Fe–O distance) and magnetic results in satisfactory agreement with experiment for $[Fe_2OCl_6]^{2-}$ In addition, tests on other (smaller) bridged antiferromagnetic systems have confirmed the validity of this approach and are published elsewhere.[13]

Calculational Details

A. Geometries. The system studied is based on a molecule for which there exist experimental crystal structures and magnetic data. There are four known complexes of $[Fe_2OCl_6]^{2-}$ with different cations[10,14] for which structural and magnetic data are available (Table I). For the calculations reported here, 16 different geometries were used (Figure 1). Each Fe–Cl distance was chosen from the experimental data to be 2.21 Å, and the local geometry around each Fe atom is nearly tetrahedral with an Cl–Fe–Cl angle of 108.94° and an Cl–Fe–O angle of 110.0°. The Fe–O bond distance (P) and Fe–O–Fe angle (θ) were varied while keeping the other pieces of the molecule fixed in the eclipsed conformation in order to obtain the dependence of energetic quantities on these specific changes in geometry. We did not consider here the staggered conformation which is also known to occur. The range of P covered is from 1.65 to 1.95 Å in increments of 0.10 Å, and θ is varied from 180 to 120° in increments of 20°. Two Na^+ ions serve as the counterions in this model to preserve charge. One Na^+ ion is placed 3.0 Å from each iron atom along the line containing oxygen and iron.

B. Basis Sets. The basis set for each Fe atom is derived from that of Hay and Wadt[15] and contains functions for the 3s and 3p orbitals along with the valence 4s, 4p, and 3d orbitals. The $n = 3$ core orbitals are included in the calculations due to their comparable size to the valence orbitals.[15] Using the coefficients from ref 15, the s orbital basis was contracted (3,4,1), the p orbital basis was contracted (3,1,1), and the d orbital basis was contracted (4,1). The Ne core was replaced by an ab initio effective potential.[15]

The oxygen basis consists of the (9s5p/3s2p) Dunning contraction of the Huzinaga basis plus a negative ion p function plus a single d polarization function.[16] The chlorine valence space is represented by a minimum basis set containing three s and three p gaussians, and the Ne core is replaced by an effective potential.[17] The sodium basis is contracted (3,1) from the Melius basis.[18]

C. Wave Functions. As described below, it is necessary to calculate the energies of two spin states to obtain Heisenberg exchange coupling constants (J). The formal electron count in $[Fe_2OCl_6]^{2-}$ gives five unpaired 3d electrons per iron center, and the ligand field around each iron favors local sextet (high-spin) coupling of the five electrons. These two centers can couple ferromagnetically to give an overall high-spin state with $S = 5$ or antiferromagnetically to yield $S = 0$ (the observed experimental[1] ground state). To obtain a wavefunction for the $S = 5$ high-spin state, an open-shell RHF calculation was used. The $S = 0$ state cannot be accurately described by a wave function consisting of only a few Slater determinants, but a broken symmetry UHF calculation[7,8] provides a useful approximation. Extracting magnetic coupling constants from the energies of these wave functions is described in the next section.

D. Heisenberg Coupling Constants. The coupling constant J can be determined by using the Heisenberg–Dirac–van Vleck spin Hamiltonian[1] ($H_{HDVV} = -2JS_aS_b$, where S_a and S_b are the spins of magnetically interacting atoms a and b) if the energies of two different pure spin states of the system are known from[7]

$$E(S) - E(S-1) = -2JS \tag{1}$$

By extension, for a ferromagnetic state ($S = S_{max}$) and an antiferromagnetic state ($S = 0$), the following is obtained:[7,8]

$$E(S_{max}) - E(S=0) = -S_{max}(S_{max}+1)J \tag{2}$$

Noodleman[7,8] has derived an expression relating the Heisenberg exchange coupling constant to the energies of the broken symmetry UHF wave function (E_B) and the high-spin state (E_H) with $S = S_{max}$. There is a certain amount of spin contamination in the low-spin broken symmetry UHF wave function (i.e., it is not a pure singlet with $S = 0$), but spin projection can be used to obtain the relationship

$$E_H - E_B = -(S_{max})^2 J \tag{3}$$

Magnetic coupling constants were calculated for each of the 16 different geometries using the energy difference:

$$J_{RU} = [E(\text{RHF high-spin}) - E(\text{UHF broken symmetry})]/25 \tag{4}$$

A key feature of this approach is that the broken symmetry UHF wave function can be related to a type of limited configuration interaction. Noodleman and Davidson[8] have shown, in the context of a spin-polarized CI treatment, that the total Heisenberg coupling constant J can be separated into a sum of terms

$$J = J_F + J_{SUP} + J_{LSP} + J_R \tag{5}$$

where J_F is the ferromagnetic contribution, J_{SUP} is the superexchange part, J_{LSP} is the contribution from ligand spin polarization, and J_R contains the remaining contributions to the total J. By representing the broken symmetry low-spin wave function as a weighted superposition of pure spin states, they showed that the J value obtained from the relationship in eq 3 contains J_F, J_{SUP}, and J_{LSP}, but not J_R.

In related work,[13] we have calculated J values for the small model bridged antiferromagnetic systems HHeH, HFH^-, and $(Cl_2Ti)_2O$ by substituting the energies from full or nearly full CI wave functions into eq 2. Assuming the Heisenberg Hamiltonian offers a good description of the spin coupling, these J values include J_F, J_{SUP}, and J_{LSP} and some or all of J_R. These numbers are then compared to the J values obtained from eq 3, where E_H was obtained from a high-spin RHF wave function and E_B was calculated from the low-spin broken symmetry UHF wave function. We also calculated J by substituting the energies of a RHF triplet and a GVB-PP(1/2) singlet into eq 2. These J values include J_F and J_{SUP} only. Good agreement between the CI and broken symmetry J values was found over a wide range of bridge-ion separations. For HHeH at 1.5 Å, a full CI gives $J = -569$ cm^{-1} and $J = -521$ cm^{-1} with the broken

(13) Hart, J. R.; Rappé, A. K.; Gorun, S. M.; Upton, T. H. *J. Phys. Chem.* **1992**, *96*, 6264.
(14) (a) Petridis, D.; Terzis, A. *Inorg. Chim. Acta* **1986**, *118*, 129. (b) Weiss, H.; Strahle, J. *Z. Naturforsch.* **1984**, *39b*, 1453. (c) Reiff, W. M.; Witten, E. H. *Polyhedron* **1984**, *3*, 443. (d) Schmidbaur, H.; Zybill, C. E.; Neugebauer, D. *Angew. Chem., Int. Ed. Engl.* **1983**, *22*, 156. (e) Drew, M. G. B.; McKee, V.; Nelson, S. M. *J. Chem. Soc., Dalton Trans.* **1978**, 80.
(15) Hay, P. J.; Wadt, W. R. *J. Chem. Phys.* **1985**, *82*, 299.
(16) Dunning, T. H.; Hay, P. J. In *Methods of Electronic Structure Theory*; Schaefer, H. F., Ed.; Plenum Press: New York; Vol. 4, 1977; Chapter 1.
(17) Rappé, A. K.; Smedley, T. A.; Goddard, W. A. *J. Phys. Chem.* **1981**, *85*, 1662.
(18) Melius, C. F.; Goddard, W. A. *Phys. Rev. A* **1974**, *10*, 1528.

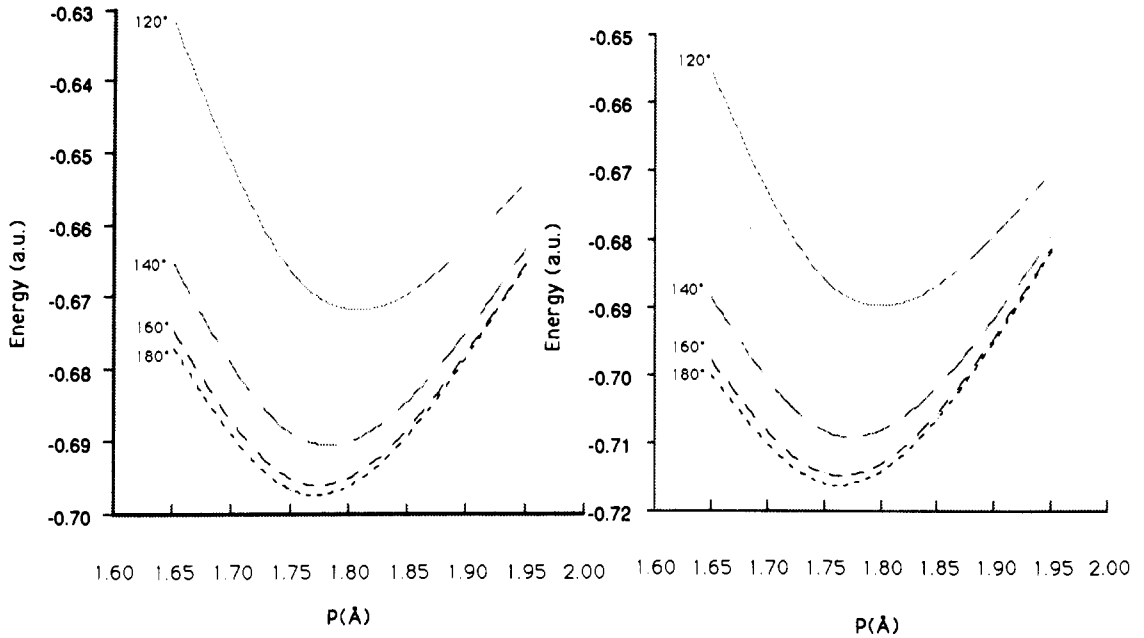

Figure 2. Energies of the (a, left) RHF high-spin and (b, right) UHF low-spin broken symmetry wave functions as a function of Fe–O distance (P) for each Fe–O–Fe angle.

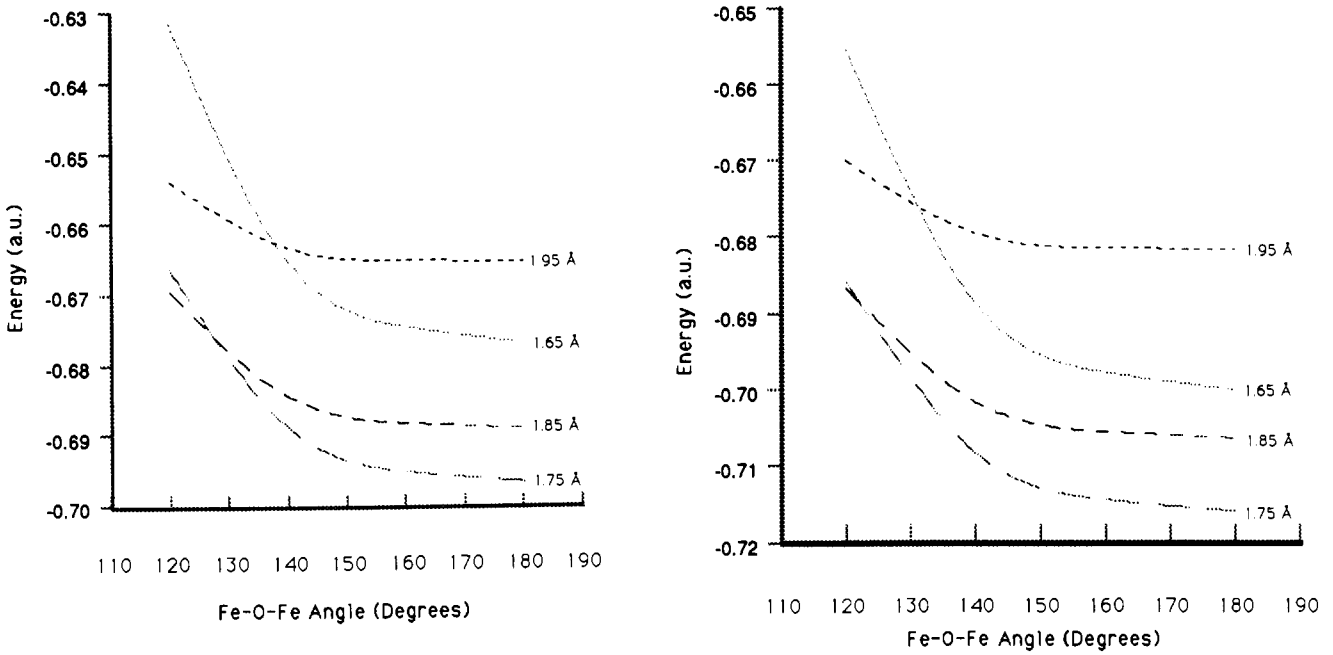

Figure 3. Energies of the (a, left) RHF high-spin and (b, right) UHF low-spin broken symmetry wave functions as a function of Fe–O angle (θ) for each Fe–O distance.

symmetry approach, and $J = -404$ cm^{-1} using the energy difference between a RHF triplet and a GVB-PP(1/2) singlet. For HFH^- at $R_{HF} = 1.875$, $J_{CI} = -863$ cm^{-1}, J broken symmetry $= -703$ cm^{-1}, and J using a RHF triplet and a GVB-PP(1/2) singlet is -327 cm^{-1}. Therefore, it is our conclusion that the broken symmetry approach (eqs 3 and 4) produces J values comparable to those which would be obtained from much larger CI calculations.

Table II. Optimum Fe–O (P) Distances in Å

wave function	θ (deg)			
	120	140	160	180
UHF	1.802	1.769	1.758	1.756
RHF	1.811	1.779	1.769	1.766

Results

A. Total Energies and Optimum Geometry. The total energies of the RHF and UHF wave functions for $[Fe_2OCl_6]^{2-}$ are plotted as a function of the Fe–O distance (P) in Figure 2 and the Fe–O–Fe angle (θ) in Figure 3. The energies of both wave functions display a similar geometric dependence. The points for each θ in Figure 2 were fitted with a cubic polynomial function, and the optimum P values were found (Table II). The energy for $\theta = 180°$ lies below the energies for the other three angles at all distances, and the Fe–O bond distance yielding the lowest energy increases as the angle decreases. The angle dependence of the energy in Figure 3 shows that the optimum angle for each P is 180°, with a sharper increase in the energy as the angle decreases for the shorter P values. The relationship between the geometric variations and the total energies is easily rationalized by considering simple nonbonded interactions. The repulsive interactions between the chlorine atoms on each iron center should force the Fe–O distance to increase as θ decreases, and this is observed. The geometries with the lowest calculated total energy are $P = 1.756$ Å and $\theta = 180°$ for the UHF broken symmetry

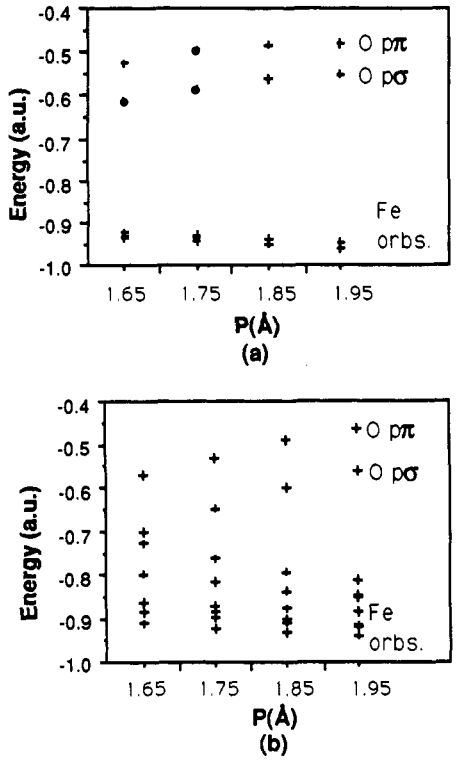

Figure 4. Orbital energy as a function of P at Fe–O–Fe = 180°: (a) Five orbitals of Fe d character and the orbitals of O pπ and pσ character with spin α from the UHF low-spin broken wave function; (b) ten orbitals of Fe d character and the orbitals of O pπ and pσ character from RHF high-spin wave function.

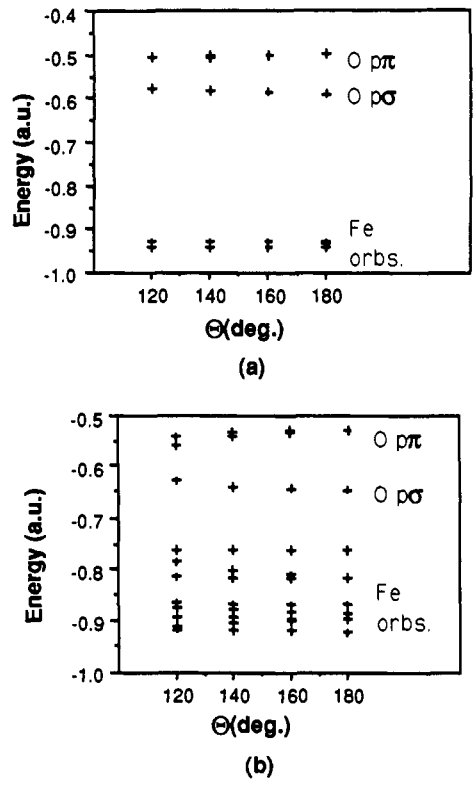

Figure 5. Orbital energy as a function of Fe–O–Fe angle at P = 1.75 Å: (a) Five orbitals of Fe d character and the orbitals of O pπ and pσ character with spin α from the UHF low-spin broken wave function; (b) ten orbitals of Fe d character and the orbitals of O pπ and pσ character from RHF high-spin wave function.

low-spin wave function and P = 1.766 Å and θ = 180° for the RHF high-spin wave function. Experimentally[10-12,14] (Table I), P covers a very narrow range from 1.752 to 1.765 Å, while θ varies from 148.1 to 180°, depending on the counterion.

B. Orbital Energies. For θ = 180°, both wave functions exhibit the same qualitative orbital energy characteristics at each distance. The orbitals of metal d orbital character lie below the p orbitals of oxygen and chlorine for both wave functions. As expected, the σ orbital (oxygen $2p_z$) is lower in energy than the π orbitals (oxygen $2p_x$ and $2p_y$) due to the higher degree of overlap in the bonding interaction with the metal. At shorter distances (Figure 4), the π-interactions with the metal become important, and all the oxygen orbitals are stabilized, the metal orbitals rise slightly in energy, and the chlorine orbitals remain aproximately constant in energy. As the Fe–O–Fe angle is decreased from 180° (Figure 5), the most notable features are that the oxygen π orbitals are slightly stabilized (and their degeneracy is broken), while the σ orbital goes up in energy.

C. Orbital Plots. The orbitals of mainly iron dσ character at P = 1.75 Å and θ = 180° are shown from the RHF high-spin wave function (Figure 6) and from the UHF broken symmetry wave function (Figure 7). The RHF high-spin orbitals are delocalized over the Fe–O–Fe fragment and display antibonding interaction between the iron centers and the oxygen. The dσ + dσ combination of iron atomic orbitals is of the correct symmetry to interact with the oxygen atomic orbital of 2s character, while the dσ – dσ combination of iron atomic orbitals contains oxygen pσ character. The UHF broken symmetry orbital of α spin is localized on the left side of the molecule as a result of the symmetry breaking, and there is also extensive delocalization to the oxygen center. The corresponding orbital of β spin is the mirror image of the α-spin orbital, with the mirror plane passing through oxygen and bisecting the Fe–Fe axis.

D. Mulliken Charge Distributions. The effective number of electrons per oxygen and iron center can be compared for the two wave functions calculated. Oxygen is most negative at P = 1.95

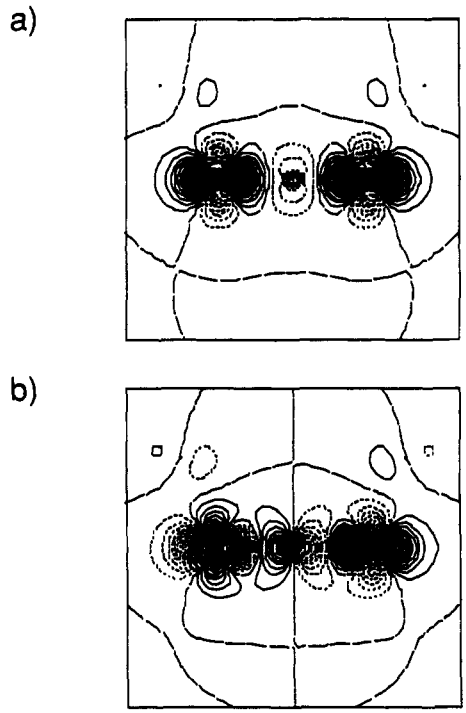

Figure 6. RHF high-spin wave function molecular orbitals from the (a) symmetric combination of Fe dσ orbitals and (b) antisymmetric combination of Fe dσ orbitals.

Å and θ = 180°, where the Mulliken population (and Mulliken charge) of the oxygen atom for both the UHF low-spin and RHF high-spin calculations are 9.1 (–1.1). When θ and P decrease, the formal charge of oxygen decreases by a very small amount to a low of 9.0 (–1.0). The general trend for the iron atoms is the opposite of that observed for oxygen. The iron centers gain

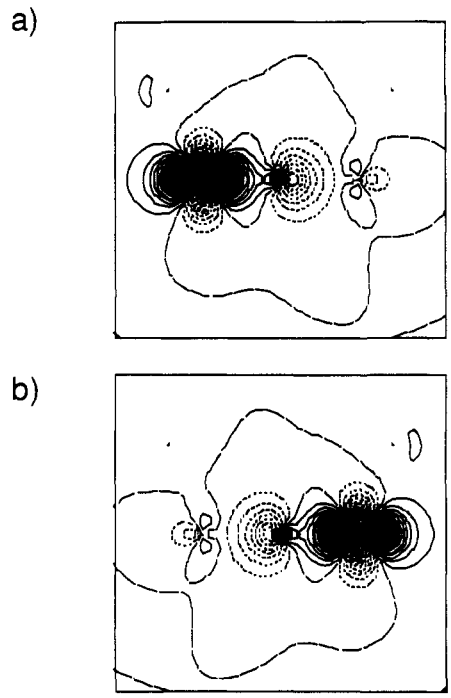

Figure 7. UHF broken symmetry low-spin Fe dσ orbital of (a) spin α and (b) spin β.

electron density as the oxygen loses it, indicating a slight increase in ligand-to-metal charge tranfer as P decreases. The maximum population (minimum positive charge) on iron occurs at P = 1.65 Å and θ = 180°: RHF high spin = 15.1 (+0.9); UHF low-spin = 15.2 (+0.8). The calculated charges are rough estimates of true charges and will tend to overestimate charge transfer; however, it should be noted that the charges are far less than the formal charges of +3 for iron, −2.0 for oxygen, and −1.0 for chlorine obtained from a formal electron count.

E. Spin Densities. For the low-spin broken symmetry UHF wave function, the calculation is performed with an equal number of α- and β-spin orbitals. The spin density on each center is roughly approximated to be the difference in the Mulliken populations over centers of the α and β orbitals. By symmetry, there is no unpaired spin density on oxygen, and α-spin orbitals gather on the left side while the β-spin orbitals gather on the right side. The spin density on the iron atoms remains constant at 4.3 for all geometries, compared to the formal electron counting value of 5.0. The chlorine atoms also have a small amount of unpaired spin density (~0.1 per atom) at all geometries. The sum of the unpaired spin density on each side of the molecule is less than 5.0, indicating some pairing of the spins via the bridging oxygen. This sum is constant as a function of angle and increases slightly from 4.7 at P = 1.65 Å to 4.8 at P = 1.95 Å, which suggests that spin density moves toward the center of the molecule as P (Fe–O distance) is decreased.

F. Magnetic Exchange. Before the calculated magnetic coupling constants are presented, the effective spin properties of the broken symmetry UHF wave function are discussed further. In the derivation[7,8] of eq 3, the relationship $\langle S^2\rangle_B = S_{max}$ is used, where $\langle S^2\rangle_B$ is the sum of the S^2 eigenvalues of the pure spin states weighted by their contributions to the broken symmetry low-spin wave function. A simple relationship[19] exists between the effective total spin eigenvalue of the UHF wave function ($\langle S^2\rangle_B$) and the overlaps of the α and β orbitals S_{ij}:

$$\langle S^2\rangle_B = \langle S^2\rangle_{s=0} + N_\beta - \sum_i\sum_j |S_{ij}|^2 \qquad (6)$$

(19) (a) Yamaguchi, K.; Toyoda, Y.; Fueno, T. *Chem. Lett.* **1986**, 625. (b) Szabo, A.; Ostlund, N. S. *Modern Quantum Chemistry: Introduction to Advanced Structure Theory*; Macmillan: New York, 1982; p 107.

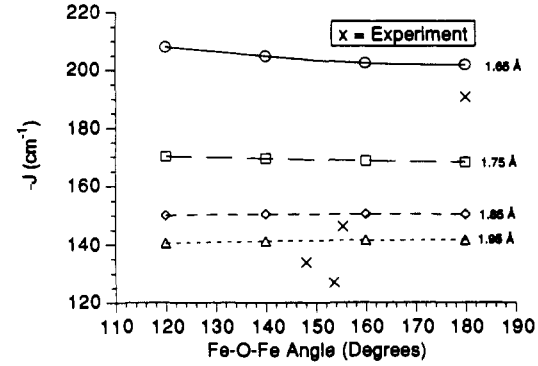

Figure 8. Coupling constants (J) of $[Fe_2OCl_6]^{2-}$ as a function of Fe–O distance for each Fe–O–Fe angle. Experimental data for $[Fe_2OCl_6]^{2-}$ salts are represented by ×'s.

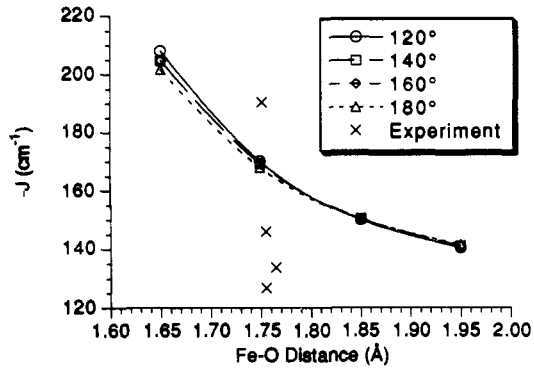

Figure 9. Coupling constants (J) of $[Fe_2OCl_6]^{2-}$ as a function of Fe–O–Fe angle for each Fe–O distance. Experimental data for $[Fe_2OCl_6]^{2-}$ salts are represented by ×'s. See also footnote 11.

Table III. $\langle S^2\rangle_B$ at Fe–O–Fe = 180

Fe–O (Å)	$\langle S^2\rangle_B$	Fe–O (Å)	$\langle S^2\rangle_B$
1.65	4.987	1.85	5.011
1.75	5.002	1.95	5.016

Here $\langle S^2\rangle_{s=0}$ = 0 for the singlet state and is N_β the number of β orbitals. The value of $\langle S^2\rangle_B$ at each distance for θ = 180° was calculated using (6). As expected, $\langle S^2\rangle_B = S_{max}$ = 5.0 at all distances (Table III), which is consistent with the notion that the broken symmetry UHF wave function can be approximated as a superposition of a set of pure spin-state wave functions. The use of (4) to calculate J is thus a simple interpolation scheme which takes into account the spin contamination in the broken symmetry UHF wave function.

The results can also be correlated to the total unpaired spin density on each side of the broken symmetry low-spin state. The total spin density of the broken symmetry wave function is zero, but a measurable amount of spin of opposite sign is localized on each side of the molecule. As the amount of unpaired spin density decreases, i.e., as it moves toward the center of the molecule, the trend is for the coupling constant to become more negative.

The results of applying (4) to determine the coupling constant J_{RU} yields a good agreement with published experimental data (Figure 8). While the experimental results (Table I) range from −126.9 to −190.3 cm^{-1}, the calculated results at P = 1.75 Å lie near −170.0 cm^{-1}, which is within this range. The plot of $-J_{RU}$ versus Fe–O–Fe angle (Figure 9) demonstrates that $-J_{RU}$ is nearly constant for all distances,[11] although there is a slight increase in $-J_{RU}$ as the angle is decreased at P = 1.65 Å and P = 1.75 Å. As a function of distance (Figure 8), the magnitude of J_{RU} increases rapidly as P is shortened.

For the geometries investigated here, the results qualitatively agree with the magnetostructural relationship recently proposed.[5] In that study, for multiply bridged oxo centers, J cannot be correlated with angular variation or with Fe–Fe distance, but it

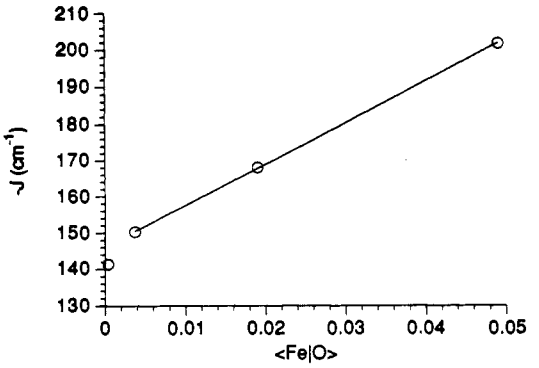

Figure 10. Plot of $-J$ versus the fourth power of the overlap between the iron $d\sigma$ orbital and the oxygen $p\sigma$ orbital from the UHF wave function.

is found to be related "exponentially" to the "shortest superexchange pathway", i.e., the shortest Fe–O bond.[5]

$$-J = A\exp(BP) \qquad A = 8.763 \times 10^{11} \qquad B = -12.663 \quad (7)$$

However, in this study, J_{RU} cannot be fit exactly by a function of the type $-J = A\exp(BP)$, where A and B are empirically determined parameters, but the plot of $-J(P)$ still shows a decrease as the distance is lengthened. As discussed elsewhere,[20] the leading terms in an analytic expression for J can be shown to depend on the fourth power of the metal–bridge overlaps and the square of the metal–metal overlaps. A plot of $-J_{RU}$ versus $\langle d_\sigma|p_\sigma\rangle^4$, where $\langle d_\sigma|p_\sigma\rangle$ is the overlap between the metal $d\sigma$ orbital and the oxygen $p\sigma$ orbital from the UHF wave function for $\theta = 180°$, shows a linear relationship (Figure 10) for $P = 1.65$, 1.75, and 1.85 Å. (The point for $P = 1.95$ Å lies slightly off this line. At infinite P, the system consists of two high-spin d^6 iron atoms and a triplet oxygen atom.[21] Inspection of the orbitals for $P = 1.95$ Å shows that this state begins to contaminate our wave functions.) Varying the Fe–O–Fe angle over a range of 60° also has very little effect. These results are qualitatively consistent with the exponential dependence of $J(P)$ suggested previously.[5]

The idea of an exponential dependence of the magnetic coupling constant is not entirely new. For example, configuration interaction calculations of the four-electron system V^{2+}–F^-–V^{2+} have been performed in an attempt to describe the distance dependence of J.[22] Several of the leading terms in the expression were found to vary as $\langle d|p\rangle^4$ (i.e., the fourth power of the overlap between a d orbital on the metal and a bridging p orbital), which behaves as an exponential function of the V–F distance.

Conclusions

There are several important conclusions which can be drawn from this work. At a conceptual level, the distance dependence of the magnetic exchange coupling constant is more important than angular dependence for singly oxygen-bridged iron(III). For a singly bridged oxodiiron(III) complex we find J_{RU} to remain almost constant over a 60° range of Fe–O–Fe angles from 120 to 180°,[23] while varying the Fe–O distance by 0.30 Å from 1.65 to 1.95 Å results in a change in J_{RU} of nearly 70 cm^{-1}. Although this distance dependence is not exactly exponential, J_{RU} increases sharply as the Fe–O distance is shortened, which qualitatively corresponds to the distance dependence found experimentally.[5] The distance dependence is also consistent with an orbital overlap picture, in which the leading terms in an analytic expression for J are found to vary as the fourth power of the overlap between the metal and ligand orbitals.

Numerically, the calculated J_{RU} results agree with the experimental results. The sign of J_{RU} is correct and the magnitudes of the magnetic coupling constants compare favorably to the reported J values for this system considering the computational and experimental limitations.

Further, it has been shown that the broken symmetry UHF approach serves as an approximation for a limited configuration interaction.[8] Calculations on other systems,[13] in which both configuration interaction and UHF broken symmetry wave functions were used, support these findings.

Finally, it is reasonable to conclude that the distance dependence of the magnetic exchange coupling constant is more important than the angular dependence for both singly and multiply bridged diiron(III) complexes. Work aimed at understanding the importance of multiple versus single bridges in mediating magnetic exchange is in progress.

Acknowledgment. A.K.R. acknowledges partial support of this research by the National Science Foundation. The authors would also like to thank Prof. Karl Wieghardt for making a preprint of his paper available.

(20) Hart, J. R.; Rappé, A. K.; Gorun, S. M.; Upton, T. H. *J. Phys. Chem.* **1992**, *96*, 6255.
(21) Hart, J. R.; Rappé, A. K. Unpublished results.
(22) (a) Shrivastava, K. N.; Jaccarino, V. *Phys. Rev. B* **1976**, *13*, 299. (b) Huang, N. L.; Orbach, R. *Phys. Rev.* **1967**, *154*, 487.
(23) For (μ-oxo)diiron(III) complexes exhibiting very short Fe–O distances an increase in J with an increase in Fe–O–Fe angle has been reported[2] for salen complexes (for $\theta = 145°$, $J = -92$ cm^{-1}; for $\theta = 173.4°$, $J = -100$ cm^{-1}). This angular dependence cannot be established within experimental errors for the $[Fe_2OCl_6]^{2-}$ system.[12] We find the opposite angular dependence for an Fe–O distance of 1.65 Å; see Figure 9.